Oceanographic Experiment Design by Simulated Annealing

NORMAN BARTH AND CARL WUNSCH

Department of Earth, Atmospheric, and Planetary Sciences, Massachusetts Institute of Technology, Cambridge, Massachusetts

(Manuscript received 23 May 1989, in final form 26 October 1989)

ABSTRACT

The oceanographic experiment design problem is discussed in the context of several simple examples drawn from acoustic tomography. The optimization of an objective function—chosen to characterize the array design—is carried out using the technique of simulated annealing. A detailed description of this method and its implementation for the examples above, is provided. Although computationally intensive, when it is carefully implemented, simulated annealing is found to give superior results to more traditional methods of nonlinear optimization.

1. Introduction

Oceanographic observations are difficult and very expensive to obtain. The problem of making the best use of available resources has been an issue for oceanographers from the earliest days of the subject. As instrumentation becomes more sophisticated and expensive, and as the complexities of the ocean system are better understood, deciding how best to use a system of instruments becomes more urgent. These questions arise in many different contexts: given (say) 8 moorings and 30 current meters, where should they best be placed to map the mesoscale in a particular region? Where should they best be placed to determine the spectrum of the zonal currents? Given a satellite whose movement obeys Kepler's Laws of motion, what orbit would best determine the wind field over the ocean? Given a computer model, what choice of grid point locations will most efficiently describe the velocity field?

We are unaware of many attempts at finding a fully systematic answer to such questions, although (as described below) some work has been done along these lines. Despite the obvious importance to a scientist working with expensive equipment, of finding the "best" place to put his instruments, most experiment design is intuitive, relying mostly upon qualitative use of sampling theorems and experience. Although the desirability of "experimental design studies" has long been discussed among modelers and observers, the actual conduct of such calculations has been few and far between. The reason for this state of affairs is easy to determine—the problem, as we will show, is a very difficult, intrinsically nonlinear one, whose solution is awkward at best, and at worst, nearly impossible. The problem is compounded by the obvious dependence of its answer upon the willingness of the observer to state in quantitative terms the precise goals of his observations. Quantifying such goals is neither traditional, nor easy.

The paper by Bretherton et al. (1976) was an important forward step in the direction we wish to go. Stimulated by the need to design a current meter array for the MODE program (Mid-Ocean Dynamics Experiment), they exploited the methods of objective mapping developed mainly in a meteorological context, to evaluate the efficacy of any given array for the specific purpose of drawing the best possible map of the mesoscale eddy field. This and related approaches are worth understanding in outline. They demand a statement of an objective function (in the Bretherton et al. case, a mapped field having minimum mean square expected error), as well as quantitative a priori estimates of the statistics of the observational noise, and of the field one is trying to map. (A statement of the dynamics of the field to be mapped can be substituted for its statistics.) The resulting algorithms produce very useful measures of the capability of a particular array.

The objective mapping approach is very effective, and has been often used. Its chief limitation, from our present point of view, is that it can be characterized as a "cut-and-try" approach. That is, one designs an array (we use the term "array" to denote any distribution of observations in space and time) based upon experience and intuition, and evaluates how well it does. One can compare the behavior of the array to a sequence of modifications, choosing the one that does best in terms of the objective function being used. When one is finished, one has the best array chosen from all those tried. However, there are no guarantees that some array not tried might do much better still.

Corresponding author address: Dr. Carl Wunsch, M.I.T., EAPS 54-1524, Cambridge, MA 02139.

So the problem one wishes to solve is as follows: Given an objective function, an explicit set of resources (shiptime, a fixed number of current meters, or of tomographic instruments, etc.), a statement of the dynamics (or statistics) of the unknown field and of the observational errors, what is the best possible deployment strategy? This is an optimization problem.

It is the purpose of this paper to lay out a general statement of the experimental design problem, and to explore its solution, primarily by working through examples. The examples chosen are from ocean acoustic tomography, and the method we will use is called "simulated annealing." However the main intention is to demonstrate the nature of the general problem, and to show that a number of methods can be adapted to its solution.

In this paper we will examine the design of acoustic tomographic arrays (for the two horizontal dimensions only). These experiments which typically seek to map the mesoscale characteristics of the ocean in all three dimensions, suffer from a lack of data. For exactly this reason it is desirable to design acoustic arrays with much care. The question we seek to answer is where should the sources and receivers (or transceivers) be located in an acoustic tomographic array.

Similar investigations have been undertaken in the context of objective mapping by Bretherton and McWilliams (1980). They sought the optimal array configurations of N instruments which would answer the following questions: 1) How well can some field $\phi(x)$ be interpolated between observation points? 2) What are the covariance functions for the errors in the mapped field? and 3) If $\phi(x)$ also varies in time, and time series are measured at each observation point, what is the best estimate of the frequency and wave number spectrum for the field ϕ? Their approach to the design problem, and their choice of objective function, was one based on statistics and information theory. However, they did not actually design any arrays.

Kumar and Seinfeld (1978) discuss measurement location in the context of optimal control theory, and seek positions which minimize the upper bound of (for finite dimensional systems) the trace of the covariance matrix. They designed optimal arrays for two observation points along a (one dimensional) bar whose heat conduction properties are described by the diffusion equation with a linear sink term (the bar lost heat to the surroundings).

Schröter and Wunsch (1986) employed a method closely related to those of control theory (although their vocabulary is different). A set of Lagrange multipliers was used to impose a general circulation model as dynamical constraints on the optimization of an objective function. The mapped values of the Lagrange multipliers then determine the regions of greatest objective function sensitivity to particular measurement types. The best observational strategy depends both upon the objective function and the particular model.

Bennett (1985) chooses an objective function similar to that of section 3 (below) to characterize fixed acoustic tomographic arrays. Using this function, he evaluates a small set of intuitively designed arrays, and their ability to map—through inverse methods—a (simulated) continuous field.

The choice of objective function represents an important element in the array design problem. Langstaff et al. (1987) noted that the design of an air monitoring network which achieves lower error variances will usually be different from a network which seeks to estimate human exposure to toxic air. However, any choice of objective function, and the array design it gives rise to, results in compromises of various characteristics of the experiment (Eisler et al. 1982).

Measurement array design is clearly a nonlinear "optimization problem." Such problems are difficult and there is a great deal to be learned about how to solve them in practice. The purpose of the present paper is to explore one particular approach, an essentially stochastic one, by tackling realistic array design issues.

To produce specific examples, the 1981 fixed array experiment of Behringer et al. (1982), and the Greenland Sea moving ship experiment of Cornuelle et al. (1988) are reexamined. Behringer et al. sought to map the mesoscale eddy structure within a 300 km × 300 km square southwest of Bermuda. The tomographic array consisted of four acoustic sources and five receivers, all moored at midwater depth on the periphery of the 300 km × 300 km square (see Fig. 1). The three-dimensional eddy fields were reconstructed from measurements of the fluctuations of the acoustic travel time

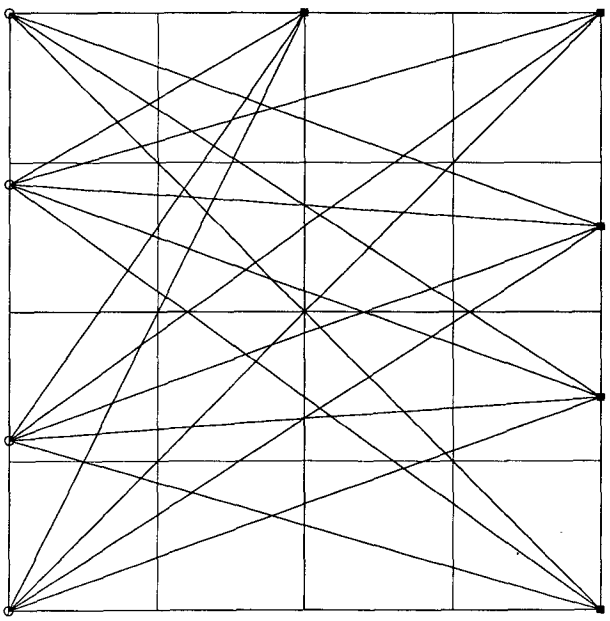

FIG. 1. The original array configuration of Behringer et al. (1982). Circles denote the locations of the acoustic sources. Black squares are the receiver locations.

between all source and receiver pairs, using inverse theory. In our revisitation of this experiment three types of fixed arrays are designed: 1) source and receiver locations constrained to be on the periphery of the region of interest, 2) receiver locations constrained to be on the periphery, and 3) source and receiver locations completely unconstrained.

The Greenland Sea moving-ship tomography experiment, sought to map the mesoscale sound speed field of the ocean within a 1000 km × 1000 km square. Moving ship tomography increases the number of acoustic rays passing through the volume of interest by having a shipborne receiver (or source) moved about a configuration of moored acoustic sources (or receivers—see Fig. 2). Computer simulations by Cornuelle et al. suggest significant reductions in the residual variance of the speed of sound field when compared to objective mapping of CTD data requiring similar amounts of ship time. For the moving ship tomography we design arrays with one, two, three and four sources.

2. Theory

Central to acoustic tomography is the travel time equation:

$$T = \int_\Gamma ds C^{-1} \tag{2.1}$$

where T is the time it takes for the acoustic signal moving with speed of sound $C(x, y, z)$, to travel a path Γ from a source to a receiver. A tomographic problem consists of determining C from measurements of T.

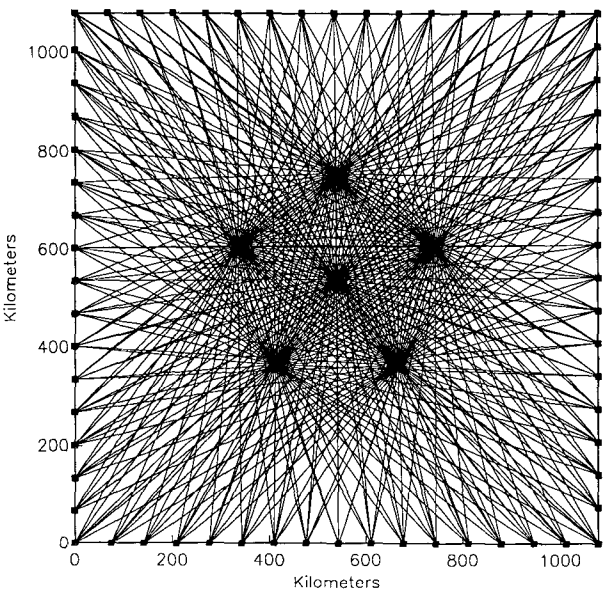

FIG. 2. The configuration of acoustic sources used in the Greenland Sea moving ship experiment (Cornuelle, Munk, Worcester 1989). Circles are as in Fig. 1; black squares are ship stations.

If the reference speed of sound is taken to be C_o, then any fluctuations in the speed of sound will produce fluctuations in the measured travel times which can often be linearized to

$$\Delta T = -\int_T ds C_o^{-2} \Delta C. \tag{2.2}$$

One needs a model ocean to proceed further. A simple, but useful, one is that of Munk and Wunsch (1979) who broke the ocean up into a set of squares (pixels), each of which is assumed for simplicity to have a constant speed of sound fluctuation such that Eq. (2.2) becomes

$$\Delta T_i = -\sum_{j=1}^{N_M} \mathbf{A}_{ij} C_o^{-2} \Delta C_j \tag{2.3}$$

where $\mathbf{A}_{ij}$ is the length of the ith ray of the jth pixel (see Fig. 1). Absorbing the reference speed of sound and minus sign into $\mathbf{A}$, (2.3) is

$$\mathbf{A}\Delta C = \Delta T \tag{2.4}$$

where we now seek to invert (2.4) to obtain values for the model parameters ΔC. In this simple formulation of the problem, there are no noise or other error terms in the measurements. In their absence, a fully determined system would give rise to perfect resolution and a zero solution error covariance matrix; all of the model parameters would be determined perfectly.

In most cases however, the matrix $\mathbf{A}$ is singular, and instead of determining the model parameters, one is forced to estimate them. Using the singular value decomposition of A, one particular estimate for the model parameters is

$$\Delta \hat{C} = \mathbf{V}\mathbf{\Lambda}^{-1}\mathbf{U}^{\mathrm{T}}\Delta T \tag{2.5}$$

where—in the usual way—$\mathbf{U}$, $\mathbf{V}$, $\mathbf{\Lambda}$ are such that (Lanzcos 1961):

$$\mathbf{A} = \mathbf{U}\mathbf{\Lambda}\mathbf{V}^{\mathrm{T}} \tag{2.6}$$

and where it is understood that the zero singular values and corresponding null space vectors in Λ have been suppressed.

In general, even without noise, if $\mathbf{A}$ is not of full rank, there is a null space and an infinite number of solutions, each of which corresponds to a particular choice of an arbitrary multiple of some set of null space vectors which satisfy $\mathbf{A}\mathbf{V}_i = 0$ (where i ranges over those values for which the singular values are either zero, or set equal to zero). That is, when $\mathbf{A}$ is of rank p ($<N_M$ the number of model parameters) then there is a null space and the vector of model parameters breaks up into a piece ΔC_p which is determined by $\mathbf{A}$ and a piece which lies in the null space ΔC_o about which no information is available. The matrix $\mathbf{V}$ also decomposes into $\mathbf{V}_p$ made up of the first p columns of $\mathbf{V}$ and $\mathbf{V}_o$ which is constructed from the columns $(p+1)$ through

N_M of $\mathbf{V}$. Then all solutions for ΔC are now of the form:

$$\Delta C = \Delta C_p + \mathbf{V}_o \boldsymbol{\alpha} \tag{2.7}$$

where $\boldsymbol{\alpha}$ is a matrix of arbitrary coefficients. Recalling the orthogonality properties of the columns of $\mathbf{V}$, (2.4) is now:

$$\mathbf{A}\Delta C_p = \Delta T \tag{2.8}$$

because $\mathbf{A}\mathbf{V}_o = \mathbf{U}_p\boldsymbol{\Lambda}_p\mathbf{V}_p^{\mathrm{T}}\mathbf{V}_o = 0$. Different estimators of ΔC make different choices for the formally indeterminate values of $\boldsymbol{\alpha}$, ranging from setting them to zero—for the minimum mean square solution—to employing a priori statistical information about the solution. In this latter case, $\boldsymbol{\alpha}$ is chosen so that the sum of the two terms in (2.7) conforms as closely as possible to the a priori statistics.

If noise is included, equation (2.4) becomes

$$\mathbf{A}\Delta C + \Delta T_N = \Delta T. \tag{2.9}$$

The best linear unbiased estimator (BLUE) for a full rank system continues to be of the form (2.5) (Munk and Wunsch 1979; Seber 1977). The error covariance matrix is

$$\mathrm{cov}\Delta\hat{C} = \sigma^2_{\Delta T_N}\mathbf{V}\boldsymbol{\Lambda}^{-2}\mathbf{V}^{\mathrm{T}} \tag{2.10}$$

where we assume for simplicity that $\sigma_{\Delta T_N}$ has the form:

$$\langle(\Delta T_N)_i(\Delta T_N)_j\rangle = \sigma^2_{\Delta T}\delta_{ij}. \tag{2.11}$$

The resolution matrix of the model parameters is

$$(\mathrm{res}\,\Delta C) = \mathbf{V}\mathbf{V}^{\mathrm{T}}. \tag{2.12}$$

The ith diagonal element of the resolution matrix equals the estimate of the ith model parameter when the true value is unity. The trace of the resolution matrix is also easily shown to equal the number of singular values in the spectrum of $\mathbf{A}$ (where by spectrum the set of singular values of $\mathbf{A}$ is meant). Equation (2.12) is a measure of the missing information represented by $\boldsymbol{\alpha}$ in (2.8).

Another solution follows by considering the minimum variance estimator. If the a priori covariance matrix associated with the true model parameters ΔC is written

$$\mathbf{R} = \langle(\Delta C_i)(\Delta C_j)\rangle = \sigma^2_{\Delta C}\delta_{ij} \tag{2.13}$$

then the estimator which minimizes the trace of the covariance matrix is

$$\Delta\hat{C} = \mathbf{R}\mathbf{A}^{\mathrm{T}}(\mathbf{A}\mathbf{R}\mathbf{A}^{\mathrm{T}} + \sigma^2_{\Delta T}\mathbf{I})^{-1}\Delta T \tag{2.14}$$

and has covariance:

$$\mathrm{cov}\Delta\hat{C} = \mathbf{V}\boldsymbol{\Lambda}(\boldsymbol{\Lambda}^2 + \sigma^2_{\Delta T}/\sigma^2_{\Delta C}\mathbf{I})^{-2}\boldsymbol{\Lambda}\mathbf{V}^{\mathrm{T}}. \tag{2.15}$$

Which of the two estimators above, or of the many others possible, one chooses is motivated by exactly which measurement one is interested in making, and how the experiment was designed to perform this measurement. For present purposes the two estimators above are taken to be representative of the behavior of the measurement process in the presence of noise, small singular values, or both. We use these relations when we choose an objective function which characterizes a given fixed array configuration below.

3. Characterizing the fixed array configurations: Choosing an objective function

Many choices must be made when designing an experiment, and any particular set of choices will usually result in an experiment which performs particularly well in one way, to the detriment of another. However, one eventually chooses to characterize or evaluate a particular experimental configuration, it is unlikely in all but the most simple, or uninteresting, of experiments, that one choice of objective function ever properly encompasses all the possible design parameters which are interesting or relevant. For our purposes here, consider Eqs. (2.5), (2.10), (2.14), and (2.15), which are representative choices for an acoustic array experiment.

Consider the dependence of $\mathrm{cov}\Delta\hat{C}$ on the singular value spectrum of $\mathbf{A}$ given in (2.10). If there are very small singular values in $\boldsymbol{\Lambda}$, then at least some entries in $\mathrm{cov}\Delta\hat{C}$ will be extremely large. Associated with these entries will be certain elements of the estimate $\Delta\hat{C}$ which will be poorly determined, possibly unacceptably so. Similarly, from (2.14) and (2.15) we see that considerations of noise in the measurements will also be important. Although the instability of the estimate (2.5) is reduced by permitting bias, it is now important to consider the relative magnitudes of the small singular values to that of the noise term in the denominator of (2.15) (hereafter referred to simply as the noise level). Although the matrix $\mathbf{A}$ may be such that the system is fully determined, its smaller singular values may be so small that they become negligible when compared to the noise level in the measurements. In this case, it is usually better to reduce the rank of $\mathbf{A}$. Truncation of small singular values leads to a more stable estimate for the speed of sound fluctuations, but at the price of resolution loss. As mentioned in section 2, the trace of the resolution matrix equals the rank of $\mathbf{A}$. Therefore truncation of singular values will lead to deterioration in the resolution matrix. We return to this discussion when we consider designing arrays which result in systems which are underdetermined.

In designing the array, it would seem reasonable then to try to make the rank of $\mathbf{A}$ equal to the rank of the system (i.e. the number of model parameters N_M), and the magnitude of the smallest singular value in the spectrum of $\mathbf{A}$ as large as possible. If it is large enough—so that it is not noise dominated—then truncation would be unnecessary. The covariance (2.10) for the estimate (2.5) would be well behaved, and the model

resolution would not be compromised. The estimate (2.14) and its covariance (2.15) would also not be noise dominated.

Therefore one useful objective function by which to design the array would seem to be the following. Let N_M be the number of model parameters, and the singular values of **A** be given by the set $\{\lambda_i: 1 \leq i \leq p\}$ where $p \leq N_M$ is the rank of **A**, and the λ_i are ordered with λ_1 the largest and λ_p the smallest. If we desire to design a system which is fully determined then we choose F, the objective function to equal the singular value λ_{N_M}. The singular values of **A** in turn are related to how the acoustic rays pass through the boxes which make up the array, which is determined by the locations of the acoustic sources and receivers (cf. the definition of **A** given in section 2). Let a particular set of these locations be denoted by $\alpha_1 = (x_i, y_i)$ [source locations are given for $0 < i \leq n_s$ and receiver locations for $n_s < i \leq (n_s + n_r)$]. Then the objective function—when a fully determined system is desired—is simply:

$$F(A(\alpha_1)) = F(\alpha_1) = \lambda_{1,N_M}. \tag{3.1}$$

The function F is nonlinear in the set of source and receiver locations α_1. The spectrum of **A** can be obtained by finding the roots to a polynomial of the same rank of the system N_M. In the Appendix the spectrum of **A** for a simple model with only two boxes is calculated explicitly. The array design problem is to find the set of source and receiver locations α_{optimal} which maximizes F.

In section 7 below the underdetermined case is considered when perfect resolution of all the model parameters is not required. The objective function is modified to

$$F(A(\alpha_1)) = F(\alpha_1) = \lambda_{1,p} \tag{3.2}$$

where p is less than N_M and equal to the rank of **A** which is desired. Additional conditions imposed on the optimization are discussed in section 7.

4. Optimization

a. Simulated annealing

Simulated annealing was introduced by Kirkpatrick et al. (1983) to solve problems in combinatorial optimization. This optimization technique, as the name implies, attempts to find the "ground state" of a function by recasting the problem in terms of the process of annealing. It is especially well suited to nonlinear or combinatorial optimization problems. Central to the method is the algorithm of Metropolis et al., described below, which was used in the early 1950s to simulate collections of atomic spins (Metropolis et al. 1953).

Simulated annealing has its origins in statistical mechanics, and in particular, in the way in which a melt is slowly cooled, or annealed, until it forms a crystal. The lower the energy state of the constituent atoms or molecules, the more regular, and stronger, the crystal. If the cooling is too rapid—so that equilibrium conditions are not always maintained—a regular crystal does not form and the total energy of the system is not a minimum.

Searching for the global minimum of an objective function is analogous to the process of annealing. The objective function is the analogue of the energy function, which we seek to minimize. Particular values for the arguments of the objective function correspond to a particular arrangement of atoms in the crystal. The Boltzmann distribution

$$P(E_2 - E_1) = e^{-(E_2-E_1)/T} \tag{4a.1}$$

governs the probability with which one energy state is accepted over another. Given two values of the objective function, E_1 and E_2, the state E_2 is accepted over E_1 with a probability given by (4a.1), where the control parameter T corresponds to the temperature. If E_2 is less then or equal to the old value E_1, then E_2 is always "accepted." If however E_2 is greater than E_1, it is still accepted with a probability given in Eq. (4a.1). This is the heart of the Metropolis algorithm. "Downhill" moves in energy are always accepted, but sometimes "uphill" moves are as well. As the temperature is lowered the "uphill" choices becomes less likely. When the temperature is zero, only "downhill" moves are accepted.

Following some annealing schedule, T is decreased, until the minimum energy state is reached. However this is necessarily true only if T is lowered so that equilibrium is maintained (Geman and Geman 1984). Typically this rate is too slow to be computationally practical (see 4b.5). Despite this shortcoming, successful minimization has been obtained with annealing schedules which are faster than the one which guarantees convergence to the global minimum.

b. Specifics

For the fixed array design example, the array is characterized by the singular values of the matrix **A** in Eq. (2.3). If the rank of **A** is to be less than N_M the objective function chosen is (3.2). We drop the subscripts N_M and N and simply consider λ_1 associated with the set of source and receiver locations α_1. Another set of locations would be denoted α_2 and the value of $F(\alpha_2)$ simply λ_2.

To use simulated annealing it is necessary to introduce a function or routine which we called the "jump" routine (another often used name is "move"). Given a set of locations α_1 we obtain another set of locations α_2:

$$J(\alpha_1) = \alpha_2. \tag{4b.1}$$

Depending on the function one is trying to optimize, J may be a function of other parameters (such as the temperature) as well.

Consider the case where the locations of the sources and receivers are completely unconstrained. The array elements are free to take positions anywhere on the periphery, or in the interior of the area of interest. For this case, the simplest implementation of the routine J that we used is the following: the set α_2 is obtained from α_1 by first choosing one of the array elements at random, and then "jumping" it plus or minus a certain distance in either the x or y directions. The maximum distance, $d_{\max}$ it can jump decreases with the temperature T. The actual distance jumped is equal to a random fraction of this maximum distance. Thus given the ith array element in the set α_1 the ith element in the new set α_2 was

$$x_{2i} = \pm d_{\max} T r x_{1i} \qquad (4b.2a)$$

$$y_{2i} = \pm d_{\max} T r y_{1i} \qquad (4b.2b)$$

where r are random numbers between zero and one, and $d_{\max}$ is the total width (or height) of the area of interest. For the Behringer et al. (1982) array this distance is 300 kilometers. The "+" or "−" in the equations above is chosen randomly for each jump. If the new location is outside of the periphery of the area of interest, then $d_{\max}$ is added or subtracted from the new coordinates x_{2i} or y_{2i} appropriately. A check is made to be sure that this new location is not occupied by another array element. If the location is occupied, the array element is "re-jumped" from its original location again. The objective function is then evaluated for this new array configuration α_2, and we obtain λ_2. Note that if α_2 is chosen at random so that it is completely unrelated to the initial configuration α_1 then one performs nothing more than a random search through the range of the objective function. When the array elements were constrained to the periphery a similar jump routine was used, but with appropriate modifications.

As we want to maximize (rather than minimize) F, a minus sign is introduced in the exponent of (4a.1). If λ_2 is larger than λ_1 the new array configuration α_2 is accepted. If it is less than λ_1 then given the temperature T_k (see (4b.4) and (4b.5) below), it is accepted with probability:

$$P(\lambda_2 - \lambda_1) = e^{(\lambda_2 - \lambda_1)/T_k}. \qquad (4b.3)$$

Computationally, this decision is easily accomplished by generating a random number between zero and one and comparing it to $P(\lambda_2 - \lambda_1)$. If it is less than $P(\lambda_2 - \lambda_1)$ the new array configuration is accepted. If the configuration α_2 is accepted then the set of locations α_2 becomes the new argument α for the jump routine J. Otherwise the array configuration α_2 is rejected and α_1 is used again as the argument for the jump routine J.

The annealing schedule used was very simple. The temperature was reduced by a factor Δ_T such that at the $(k+1)$th iteration:

$$T_{k+1} = \Delta_T T_k. \qquad (4b.4)$$

The temperature was stepped after a certain number (N_1) of array configurations had been evaluated, or after a certain number (N_2) of array configurations had been accepted, whichever occurred first. Typical values for N_1 and N_2 were 100 and 50, respectively. The parameter Δ_T was chosen by experimentation to range from 0.95 to 0.995.

Eventually further iterations and steps in temperature fail to produce any new values for the objective function, and convergence is said to have been obtained. If the final value to which the objective function converged is λ_{conv} and if it is a true global maximum of F, then the optimal array configuration is α_{conv} associated with the singular value decomposition of the matrix **A**.

The jump routine J and the annealing schedule are problem specific, and are usually chosen through experiment. The annealing schedule necessary to guarantee convergence to a global maximum requires that as the number of iterations tends to infinity the temperature T_k is such that:

$$T_k \geqslant \frac{c}{\log(1+k)} \qquad (4b.5)$$

where c equals the difference between the largest and smallest possible values for the objective function. Typically c is too large to seriously consider using (4b.5). For example if T_k is 0.05 and c equals 1.0, then the number of iterations necessary to reach the temperature T_k is roughly 10^8. Depending on the time necessary to evaluate the objective function, the computational burden of this number of iterations quickly becomes unacceptably high. Sometimes smaller values than theoretically necessary are used for c instead. Despite this choice good convergence has been observed (Geman and Geman 1984). For our particular problem, the annealing schedule (4b.4) above gave better results after fewer iterations than logarithmic schedules. A further embellishment was to change Δ_T so that at low temperatures T decreased more slowly.

We described above our simplest implementation of a jump routine. However better results are obtained when the jump routine J was given by (4b.2) for high temperatures and by

$$x_{2i} = \pm d_{\max} T_o r x_{1i} \qquad (4b.6a)$$

$$y_{2i} = \pm d_{\max} T_o r y_{1i} \qquad (4b.6b)$$

for temperatures below T_o. A typical value for T_o (obtained after experiment) was 0.125.

It is conceivable that moving the location of just one array element will not be enough to get out of a local minimum of the objective function. Perhaps two or more sources or receivers must have their locations altered in order for $F(\alpha)$ to take on a value λ which is accepted by the Metropolis algorithm. Therefore, if $F(J(\alpha_1)) = \lambda_2$ was not accepted then this state was jumped again so that

$$F(J(J(\alpha_1))) = F(J(\alpha_2)) = F(\alpha_3) = \lambda_3. \quad (4b.7)$$

Then λ_1 and λ_3 were the new arguments to the Metropolis algorithm. If the configuration α_3 was not accepted, then it was jumped again. If no acceptable configurations were obtained, this continued up to as many times as there were array elements. After that the process was started again from the original configuration α_1. Through experimentation it was discovered that considering up to the λ_3 level did enhance convergence. Beyond this however, led to an increase in computational load together with *degraded* convergence properties.

Does simulated annealing actually find the global maximum of the objective function F above? One is guaranteed to have the global maximum if the annealing schedule is of the form given in (4b.5), but this schedule is not computationally practical in most cases. Given that the annealing schedule (4b.4) together with the modifications mentioned just above, does not guarantee that the global maximum will be found, what confidence do we have that the value λ_{conv} which the annealing program converges to is the global maximum we seek? In general it is as difficult to answer this question unambiguously as it is to find the global maximum. However, we instituted the following simple consistency check in the simulated annealing runs. A necessary condition (though not sufficient) for the global maximum of the objective function F is that it equal the largest value of F ever found during the annealing process. (Remember that configurations which degrade the current value of F are sometimes accepted by the Metropolis algorithm.) If the largest value of F obtained during an annealing, $\lambda_{\max}$, is set aside, then this should equal λ_{conv} after convergence is obtained. It is then at least true that the largest maximum of all of the local maxima which were visited was obtained by the annealing. If one of these corresponds to the global maximum then one is done. Note that due to the random "Monte Carlo" nature of simulated annealing, the starting point of the annealing process is irrelevant. At high temperatures, steps in the objective function are readily accepted whether they be "uphill" or "downhill" (see Fig. 3), and the memory of where the annealing process started is quickly lost.

The computational load of simulated annealing can be quite high. For the case where all array elements were constrained to locations on the periphery, convergence was obtained after roughly 400 iterations (i.e. after at most 400×100 evaluations of the objective function). When the possible array element locations were completely unconstrained convergence was obtained after roughly 4200 iterations. Thus computer run times varied from a few hours to several days on a SUN 3/50 with floating point coprocesser. No serious attempt was made at making the annealing code run as fast as possible. Within the annealing context however, there are various things one can do to increase the speed of execution. For example, given that $J(\alpha_1)$ jumps one array element (say the ith) then only those acoustic rays associated with the position of the ith array element are changed. Therefore only those rows of the matrix **A** of (2.3) need be recalculated. The other rows remain unchanged.

(Although unimportant for the objective function F chosen above, it is valuable to remember that only the *difference* $(\lambda_2 - \lambda_1)$ is important for the Metropolis algorithm. In many cases calculating the difference of the two "states" of F is computationally faster than calculating the two individual values of F itself. A simple example of this is the following. If—for example—an objective function F were equal to the sum of the x and y coordinates of the locations of the array elements, then:

$$F(\alpha_1) = \sum_{i}^{(n_s+n_r)} (x_{1i} + y_{1i}) \quad (4b.8)$$

and similarly for $F(\alpha_2)$. Thus if the kth element has been moved it can be shown that

$$F(\alpha_2) - F(\alpha_1) = (x_{2k} + y_{2k}) - (x_{1k} + y_{1k}). \quad (4b.9)$$

Calculating (4b.9) directly is computationally much easier than redoing the sum in (4b.8) to find $F(\alpha_2)$ before evaluating (4b.9). Unfortunately calculating the difference $(\lambda_2 - \lambda_1)$ *directly* in analogy with (4b.9) for two simply related configurations α_1 and α_2 does not seem possible.)

5. The original acoustic array

For comparison purposes the fixed tomographic array of Behringer et al. is shown in Fig. 1. As in section 2, the simple ocean model we impose is made up of a 4 by 4 grid of squares (The model of Behringer et al. was different). The speed of sound fluctuations are assumed to be constant within each square.

The spectrum of singular values associated with the matrix **A** for this array is displayed in Fig. 4a. This array is of rank 14, with a smallest singular value of $0.013LC_o^{-2}$ where L is the length of the side of one of the boxes. In the original experiment L was 75 km. The covariance matrix for the model parameters, calculated via (2.10), is poor (Fig. 4b). The trace of this matrix is of order $10^3 C_o^4 L^{-2}$ so that the average standard deviation of each of the sixteen model parameters is roughly 200 m s^{-1}. This value is much larger than the magnitude of the expected speed of sound fluctuations.

Following the discussion of section 2 it is important to compare the size of this singular value to the expected magnitude of noise in the measurements. From Munk and Wunsch (1979) we take as a typical range for $\sigma^2_{\Delta T}$ to be from 0.1 s^2 to 0.01 s^2. A value for $\sigma^2_{\Delta C}$ is based on the change in sound speed associated with a change of 1°C at 1000 decibar. Thus $\sigma^2_{\Delta C}$ is roughly

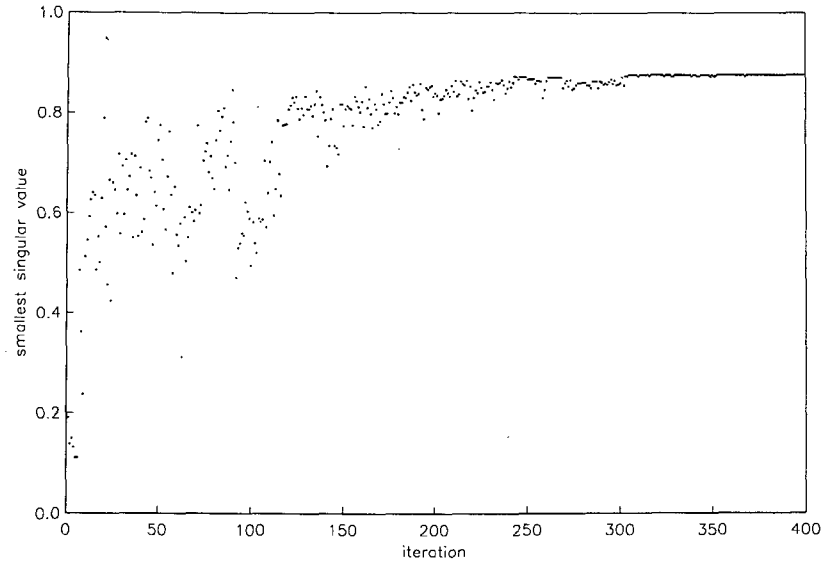

FIG. 3a. The output of the simulated annealing program when the array elements are all constrained to locations on the periphery. With each iteration along the x-axis the temperature is reduced by a factor Δ_T (typically 0.9–0.995 for the simulations here). The y-axis is the value of the objective function at each iteration. In this case it is equal to the smallest singular value of the matrix A (Eq. (2.3)) in a full rank (16) system. After roughly 400 iterations the program converges to a value of 0.876. The units for the singular values are LC_o^{-2} (C_o is the reference speed of sound and L is the length of a box side (75 km in the original experiment)).

100 $m^2 s^{-2}$. Therefore the "noise" term in (2.15) ranges from approximately 10^{-4} to 10^{-6} s^2 m^{-1}. Comparing this with the 14th singular value of the array given above (which is roughly 5×10^{-4} s^2 m^{-1}) suggests that it might be noise dominated and perhaps discarded. The 13th singular value is roughly 10 times larger than the 14th, and might be significant.

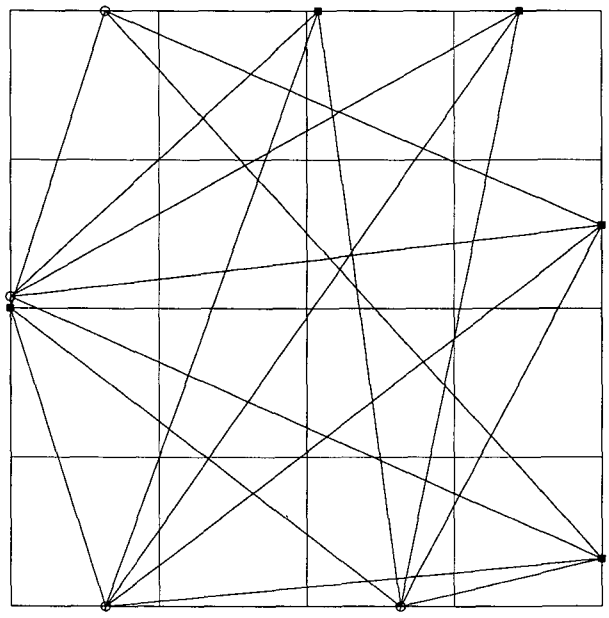

FIG. 3b. The array configuration associated with the final state of the simulated annealing program output displayed in Fig. 3a. All senders and receivers were constrained a priori to locations on the periphery.

6. Solutions

a. *The optimum fixed array with elements constrained to the periphery*

Using simulated annealing, an optimum array configuration was found for the case where all the array elements were constrained to lie on the periphery of the grid. Figure 3a displays the output of the annealing program. The final array configuration is shown in Fig. 3b. The system is fully determined and spectrum of **A** for this array is given in Fig. 4a. The N_Mth singular value is $0.876LC_o^{-2}$, a value roughly 67 times larger than the 14th, as well as one and a half times larger than the 12th, singular value of the original array. Comparison of this value with a reasonable expectation of the noise level in the measurements shows it to be roughly two orders of magnitude larger than the noise upper bound discussed in section 2. This singular value is thus not noise dominated and we can expect that the measurements associated with it are significant. As the system is fully determined, the resolution is perfect. The diagonal elements of the covariance matrix are given in Fig. 4b. The trace of this matrix is of order $10.0C^{4}{}_{o}L^{-2}$ giving an average standard deviation for each of the 16 model parameters of roughly 20 m s^{-1}.

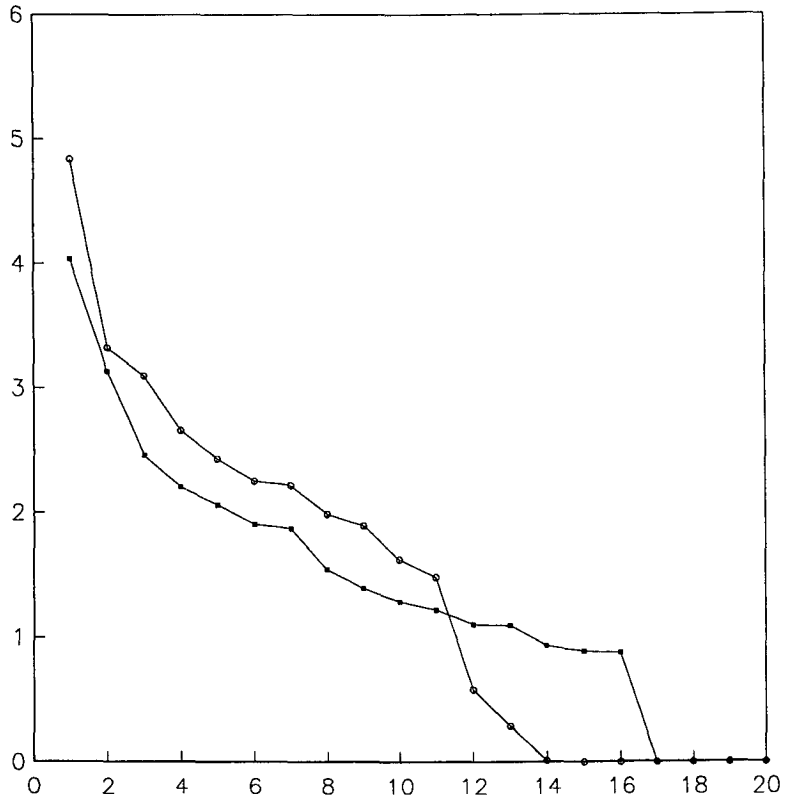

FIG. 4a. The spectra of singular values of the matrix **A** (of Eq. (2.3)) for the original array (open circles, rank 14: $\lambda_{14} = 0.012LC_o^{-2}$), and the designed array with all array elements constrained to locations on the periphery (filled squares, rank 16: $\lambda_{16} = 0.876LC_o^{-2}$). L is the characteristic length of a box side (75 km in the original array) and C_o is the reference speed of sound.

288.0 0.833	269.0 0.330	427.0 0.446	422.0 0.819
222.0 0.323	17.3 0.696	9.70 0.440	263.0 0.409
51.4 0.481	33.3 0.573	380.0 0.447	34.2 0.934
27.3 0.686	1470.0 0.476	1810.0 0.544	5.00 0.460

FIG. 4b. The diagonal elements of the covariance matrix (top numbers) for the original array configuration (rank 14), and designed array with all sources and receivers constrained to the periphery (rank 16). These give the variance for the speed of sound fluctuation in units of $C_o^4 L^{-2}$.

What is striking about the array configuration itself are the locations of S2 and R3. They are nearly on top of each other. Although the array elements have unique positions, no provision was made for insisting that they maintain a certain critical distance apart. This constraint is a practical necessity when the array design problem is extended to include the vertical dimension. Taking full advantage of multipaths requires a minimum distance between elements. Changing the locations of S2 and R3 slightly degrades the spectrum of the array. (The sensitivity of the spectrum of **A** to the weight given rays which pass along the periphery of boxes, or exactly along the interface between boxes, for this array design was found to be relatively low.)

b. The optimum fixed array with unconstrained acoustic sources

For this case, the receivers of the array were constrained to lie on its periphery, but the sources permitted to be placed anywhere within the interior, as well as on the periphery. From symmetry arguments, it is irrelevant whether one chooses the sources, or the

receivers to be unconstrained. Furthermore, because the interior of the array is now available for the placement of the sources, this additional freedom should produce an optimal array which is no worse—and perhaps better—than the array where all array elements are on the periphery.

The output of the annealing program is similar to that of Fig. 3a except that convergence takes roughly 600 iterations. The final array configuration for this case is in Fig. 5. The spectrum is such that the system is fully determined, with the smallest singular value of $0.956LC_o^{-2}$. This value is two orders of magnitude above the typical noise level we have chosen, and well above the lowest three singular values of the original array. The trace of the covariance matrix is slightly better (smaller) than for the case in section 6a above.

Permitting the acoustic sources to be located anywhere within the interior increased the computation time by a factor of roughly one and a half compared to the case when both sources and receivers are constrained to the periphery. The improvement in the maximum value of the objective function is modest and less than the factor of 1.5.

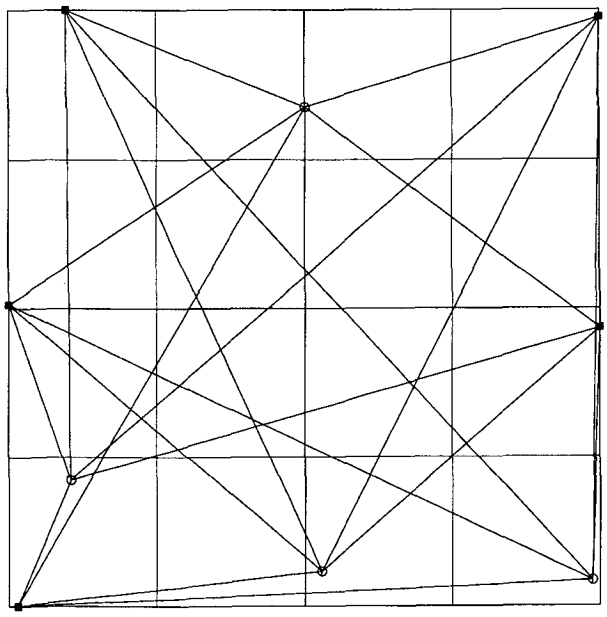

FIG. 5. The designed array configuration when only the receivers are constrained to the periphery but the sources are free to take locations in the interior.

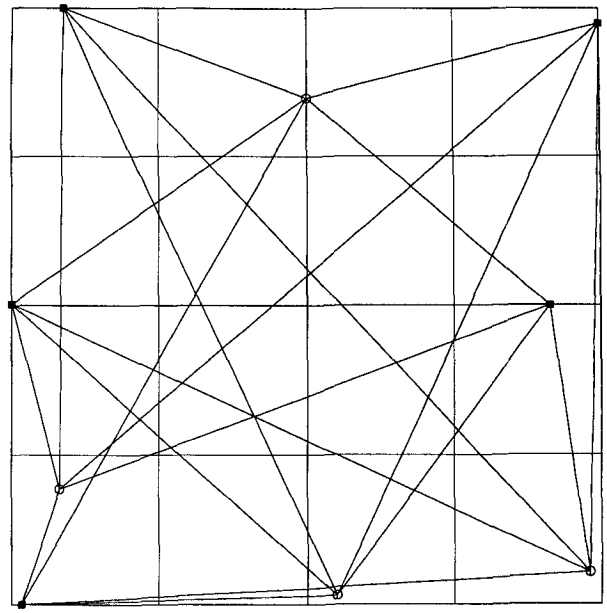

FIG. 6. The designed array configuration when the source and receiver locations are completely unconstrained.

c. The fully unconstrained optimal fixed array

In this experiment both the sources and receivers were unconstrained in their locations. The final value of the objective function λ_{conv} should be greater than or equal to the previous values of F obtained in sections 6a and 6b. The computation time increased significantly for this unconstrained case. Convergence now required roughly 4200 iterations, more than an order of magnitude longer than for the case of section 6a. The system is fully determined and possesses a smallest singular value of $0.970LC_o^{-2}$; well above the noise level. This singular value is only somewhat better than for the array of section 6b and differences in performance of these two arrays is rather small. The array configuration is displayed in Fig. 6.

If one compares this array configuration with that of section 6b there are clear similarities. Interestingly, the fully unconstrained results puts four of the five receivers on the periphery of the array, leaving only one of them in the interior. The locations of the sources for the two arrays are almost the same. The similarity of the two arrays also gives confidence that the simulated annealing program is finding a profound stationary value of the objective function. It is unlikely that two local maxima of the objective function would result in very nearly the same array configurations. This conclusion is further strengthened when one recalls that in one case the receivers are constrained to be on the periphery whereas in the other case the possible locations of the array elements are completely unconstrained.

7. Arrays with truncated spectra

Given the imposed model of boxes, the original array of section 5 was an underdetermined system. The trace of its covariance matrix was unacceptably large but if the smallest singular value in the spectrum of **A** is truncated, then the trace can be reduced by two orders of magnitude, and to within a factor of two of the traces

for the covariance matrices for the fully determined systems designed in section 6. The rank of **A** for this truncated system was 13 (recall that $N_M = 16$). Using the objective function F of (3b) we designed arrays which were underdetermined systems and also of rank 13. Due to the modest computational load when the receiver locations were constrained to the periphery and the source locations unconstrained the designed rank 13 arrays were of this type.

We considered three approaches to designing an array which is necessarily not a fully determined system. The first approach was to simply search for the array which maximized the 13th singular value, regardless of whether the higher order singular values were zero or not (in general they are not). If these singular values were not zero, they were truncated.

If the array is to be of rank 13, then a second approach accomplishes this goal if the geometry of the sources and receivers is such that no rays pass through 3 boxes of the 16 boxes. One can pick the three boxes to be excluded before any optimization of the objective function. For example, one might choose to exclude three of the four corner boxes. Then given that a particular array has no rays passing through the three corner boxes, we search for the array which has a maximum value for the 13th singular value. We know a priori that the resolution for the three excluded boxes will be zero, and the remaining 13 boxes will be resolved perfectly.

A third approach is to consider only arrays for which the higher order singular values are zero. (This was implemented in a simple and straightforward manner. Given configuration α_1 of rank 13, if $\alpha_2 = J(\alpha_1)$ is a new array of higher rank, it is discarded and $J(\alpha_1)$ is evaluated again until a rank 13 array α_3 is found such that $\alpha_2 = J(\alpha_1)$.) This approach is something of a compromise between the first two methods. No boxes are excluded a priori but there are no nonzero higher order singular values either. If the system was of rank 13, then at least 3 of the boxes will not be perfectly resolved.

Under what circumstances any of these approaches lead to the same array design is a complex question of geometry and will depend in general on which boxes are excluded and how the boxes are distributed and their size. However, it seems that these three approaches would lead to the same array design only rarely.

Not unexpectedly, λ_{conv} for the first approach was the largest of all the three designs. This is so because there were no supplementary conditions imposed on the optimization of F, as in the other two approaches. The number of iterations (1500) was also similar, or less than for the other two approaches. The designed array configuration is displayed in Fig. 7. The trace of the covariance matrix is an order of magnitude better than that of the original truncated (rank 13) array. The resolution matrix of the designed array is "mixed" with some diagonal elements being better than that of the original array, and some being poorer. In general the other two design approaches gave slightly poorer covariance matrices but all of the designs were better than the original truncated covariance matrix. A significant difference between the three approaches is to be found in the resolution matrices. The second approach above which a priori excluded three corner boxes perfectly resolved the remaining boxes, as it should. The three approach had a resolution matrix which was somewhere between that of the first two designs.

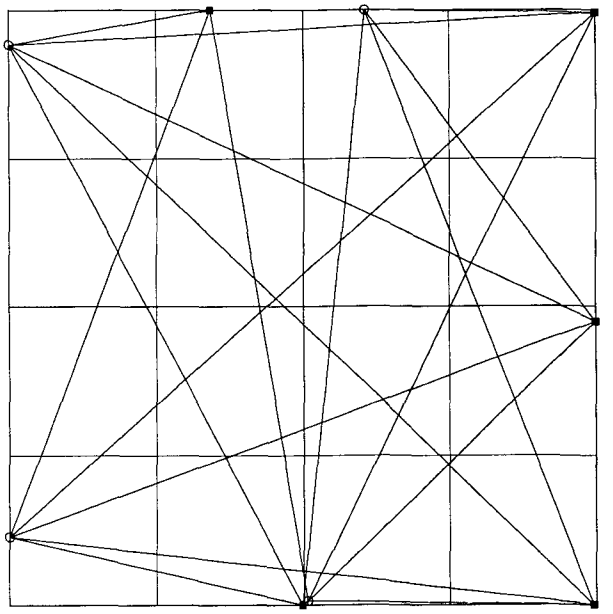

FIG. 7. The designed array configuration for an underdetermined system, with receivers constrained to the periphery.

8. Moving ship tomography

In a fixed acoustic tomographic array, the acoustic sources and receivers (or transceivers) are in a fixed configuration for the duration of the experiment. In moving ship acoustic tomography either the sources, or the receivers are now shipborne. Here it is supposed the sources continue to be moored to a particular location.

There are several conceivable advantages of moving ship tomography. The most important is the effective increase in the number of receivers. The fixed array configuration of Behringer et al. had four receivers and five sources, for a total of twenty rays (excluding any consideration of multipaths). Ship stations every 100 kilometers along the periphery of the 300 km × 300 km region of interest would, with the same number of moored sources, result in twelve receiving stations and a total of 48 rays.

Here, we revisit the Greenland Sea Tomography Experiment (September 1988–89) of Cornuelle et al.

(1988, hereafter referred to as CMW), and using their objective function, together with simulated annealing, investigate the experiment design (for the two horizontal dimensions only).

The CMW ocean model is different from the simple one posed in section 2. The speed of sound field is presumed to be expressible in terms of the first seven harmonics such that:

$$\Delta C(x, y) \sum_{kl} P_{kl} \exp[i(kx + ly)] \qquad (8.1)$$

where k and l range from -7 to 7, and are simply the harmonics of a box of side L. The coefficients P_{kl} are the desired model parameters. Using (8.1), rewrite (2.2) as

$$\mathbf{A}P = \Delta T \qquad (8.2)$$

where to first order in C_o

$$A_{mn} = \int_n ds C_o^{-2} \exp[i(k_m x + l_m y)]. \qquad (8.3)$$

The infinitesimal arc length ds is over the nth ray, and the model parameter P_m is associated with the wave numbers k_m and l_m. The covariance matrix for the true model parameters is

$$\mathbf{S}(k, l) = \langle PP^{\mathrm{T}} \rangle \qquad (8.4)$$

and is assumed to be diagonal with an exponential decay constant of 120 km. If the data error variance matrix is $\mathbf{E}$, then the minimum variance estimate of the model parameters $\hat{P}$ is (via the Gauss–Markov theorem):

$$\hat{P} = \mathbf{SA}^{\mathrm{T}}(\mathbf{ASA}^{\mathrm{T}} + \mathbf{E})^{-1}\Delta T. \qquad (8.5)$$

The matrix $\mathbf{E}$ is assumed to be diagonal and constant. The covariance matrix of the estimate is

$$\hat{S}(k_m, l_m, k_{m'}, l_{m'}) = \langle (\hat{P}_m - P_m)(\hat{P}_{m'} - P_{m'}) \rangle$$
$$= \mathbf{S} - \mathbf{SA}^{\mathrm{T}}(\mathbf{ASA}^{\mathrm{T}} + \mathbf{E})^{-1}\mathbf{AS}. \qquad (8.6)$$

These expressions, which are in wave number space, are easily transformed to ones over physical space.

The objective function used here to characterize a configuration of moorings and ship stations is then simply the rms value of the diagonal elements of the covariance matrix for the model parameters $\hat{S}$, given in (8.6). This objective function differs slightly from the original of CMW. Theirs was the fractional residual error variance $\langle (\Delta\hat{C} - \Delta C)^2 \rangle / \langle (\Delta C)^2 \rangle$, where $\langle (\Delta C)^2 \rangle$ was variously chosen to be 16 and 49 $\mathrm{m}^2\,\mathrm{s}^{-2}$.

We assume, as did CMW, that the ship stations are equally spaced around the periphery of the area of interest. The mooring locations however, are free to change within the interior.

The evaluation of the objective function above is computationally intensive. Simulated annealing requires that the objective function be evaluated many times—typically one hundred times before the temperature is stepped downward. The temperature is stepped several hundred or several thousand times, until convergence is obtained. It was not computationally possible to evaluate the full objective function with k and l taking on their full range of -7 to $+7$. The full number of model parameters had to be reduced if simulated annealing was to be used on a small computer. Neither was it feasible to have the full number of ship stations per side of the box describing the area of interest. However, a combination of reductions of these various parameters did make it possible to evaluate the objective function so that simulated annealing could reasonably be applied to the problem of designing an array.

The first case considered had only one source, which was free to take any location in the interior. The total number of ship stations was 12. These evenly spaced about the periphery of a box 1080 kms on a side (CMW typically considered 60 ship stations). The number of model parameters was 64 (CMW had 184). The final configuration was such that it placed the source at the very center of the box.

Except for the case of one source, it seems that the objective function takes on lower values when the sources are near the periphery of the array. As with the fixed array, we neglect any consideration of multipaths and have not required any minimum distance between sources and receivers.

The CMW "test bed" configuration consisted of four sources in a symmetrical arrangement a distance of 378 km from the center of the square box defining (1080 km on a side) the area to be investigated by the

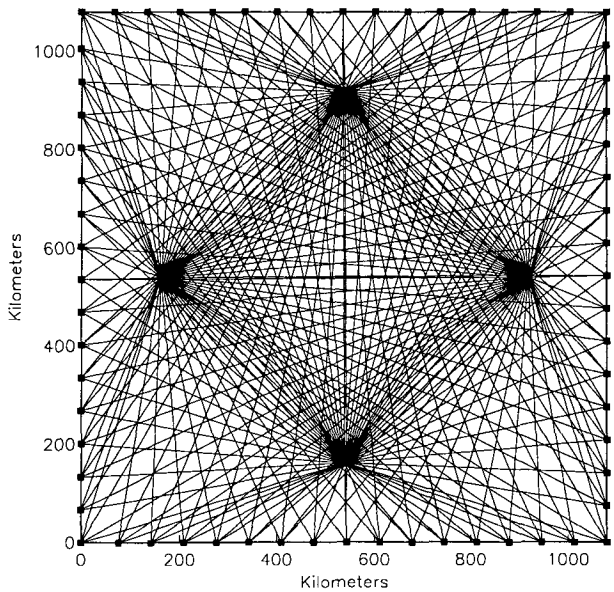

FIG. 8. The CMW "test bed" configuration (circles and squares as in Fig. 2).

array (Fig. 8). For this configuration, the average variance for each model parameter, using the reduced CMW ocean model parameters above, is 108.0 $m^2 s^{-2}$. The designed array in Fig. 9 is improved by an order of magnitude and gives an average variance of 8.0 $m^2 s^{-2}$ per model parameter. Similar improvements in the value for the objective function were obtained for the cases of two and three sources. CMW noticed that if one contours the mean square error in physical space there is unacceptably large error in the center of the array, and in their final configuration of six moored acoustic sources, one of the sources was placed in the center. The other five sources were in a pentagonal arrangement on a 216 km radius about this center. These questions were not addressed in our design which simply minimized the objective function regardless of whether this gave rise to unacceptable artifacts.

The optimization of the objective function for the moving ship tomography case—even in the reduced version we used—took significant amounts of computation time when compared to the fixed array optimizations. No serious attempts were made at optimizing the code. Three or four days of cpu time (roughly a week of real time) on an Alliant Fx/40 array processor were typical run times.

8. Discussion

The array design example of section 6c, which is a linearly constrained nonlinear optimization problem, was also tackled using more conventional non-linear optimization methods. The MINOS library (Murtagh and Saunders 1983) of optimization algorithms uses a reduced-gradient algorithm (Wolfe 1962) together with a quasi-Newton algorithm (Davidson 1959) for such problems (see also Gill et al. 1981). As with most optimization methods, the MINOS algorithm converges to the first (usually local) minimum it encounters. By starting the program at many different places one hopes to eventually encounter the global minimum.

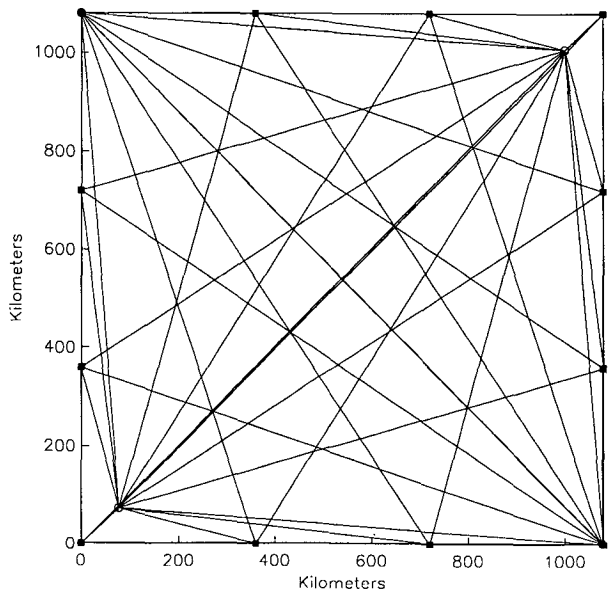

FIG. 9. The designed configuration for the acoustic sources in a moving ship experiment using a reduced CMW ocean model. Note: two acoustic sources are located at (0, 1080) and (0, 1080).

Using this strategy, several computer runs were performed to maximize the objective function F of Eq. (3.1). After more than twenty runs, all of the values to which the MINOS routines converged were less than the value obtained with simulated annealing. Many of the MINOS values were less than half that of the annealing value. These results also confirmed the suspicion that (3.1) was a complicated function with many "undulations" where conventional optimization routines would get trapped. The cumulative computational time for these MINOS runs was roughly $^3/_5$th that of the simulated annealing.

There was also an additional difficulty in running MINOS. If the initial array is of say rank 14 but we seek to design an array which is full rank (with $N_M = 16$), then the 16th singular value is zero, and —in general—so is the Hessian, as well as the gradients of the objective function. Given such an initial array, the MINOS algorithm immediately stops because all the convergence criteria are already met, although no optimal solution has been found. Essentially MINOS requires the initial configuration to be of full rank and the initial value for the objective function λ_{N_M}, nonzero. Finding such an array was a problem posed by Munk and Wunsch (1979)—a problem which they did not solve. Thus, designing optimal arrays of the kind desired in section 6 using a routine such as MINOS would not have been possible. Presumably these shortcomings extend to any optimization routine which requires the gradient, and/or the Hessian of the objective function. However this is not a problem for simulated annealing, because it is relatively insensitive to the initial choice of array. The initial array configurations used were always of a rank less then N_M.

Finally, MINOS was run using, as its initial array, the optimum array found via simulated annealing. The improvement realized in the objective function was in the fourth decimal place and not significant.

In section 7 we chose the smallest singular value of the matrix **A** as our objective function. Computer runs which maximized the ratio of the smallest to largest singular value gave rise to inferior values of this ratio than runs which simply maximized the smallest singular value. For this reason it was decided to forego this normalization.

It is also natural to ask how "robust" are the arrays designed, if one of the acoustic sources or receivers fails? This is an additional design question which was not considered in the objective functions we used. However, once objective functions which incorporate robustness criteria are chosen, designing arrays would, in principle, be straight forward.

Simulated annealing can lead to improvement over other methods of optimization. It has helped to effectively solve some of the famous outstanding problems such as the Traveling Salesman Problem (e.g., Press et al. 1986). It is especially useful when the objective function F is nonlinear and the difference between two states $F(\alpha_2) - F(\alpha_1)$ can be evaluated quickly (see section 4b). In general, enhancements to the computations one can implement are highly problem specific. However these enhancements *can* make important differences in computational tractability. The jump routine, and annealing schedule are also problem specific. The values of the various parameters associated with them are usually obtained through experimentation. In short, to run effectively, any simulated annealing program must itself first be "tuned" or "optimized." Exactly how this "tuning" is done is left entirely to the inventiveness of the person implementing the code. As simulated annealing is effectively tailored to each optimization problem, it is not possible to predict before its actual implementation what expected run times might be. Optimization problems such as the Traveling Salesman Problem are known to quickly become overwhelming computationally for ordinary optimization methods as the number of cities that the salesman must visit increases. Nevertheless, simulated annealing is able to find the shortest path—or very nearly the shortest path—after a comparatively modest amount of computation. For this reason it is, to some extent, a misunderstanding to ask how the computational load in simulated annealing will increase with the increase in the magnitude of a particular parameter (such as the number of cities). Instead, simulated annealing is simply applied where other methods of optimization offer little hope. Highly nonlinear problems with large search spaces, and combinatorial optimization are the two most often quoted examples. However, when carefully implemented, simulated annealing also offers the possibility of finding the global maximum or minimum of a general (nonlinear) function F—something few other optimization methods can claim.

A next step would be to implement these ideas in more interesting and complex contexts, such as a general circulation model. What choice of grid points best describes say the velocity field, or what at which grid points is it most important to know the wind stress? There are also important ocean state estimation questions which are hinted at in array design: where is it best to obtain additional data, and of what type, in order to best constrain a particular quantity of interest in a GCM? These sorts of questions and problems we hope to address in future work.

Acknowledgments. One of us (NB) would like to acknowledge useful conversations and interactions with N. Bindoff, I. Fukumori, P. Gaspar, and D. Rothman. This research was supported by the Office of Naval Research (Contract N00014-85-J-1241).

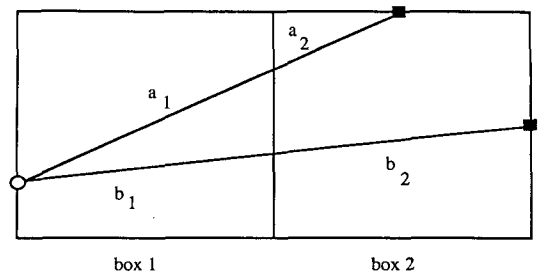

FIG. 10. A simple acoustic array of one source and two receivers imposed on a two box grid. Two rays a and b with arc lengths a_1 and b_1 transect box 1, and similarly for a_2, b_2 and box 2.

APPENDIX

An Explicit Example

A simple box model with two boxes and two rays is shown in Figure 10. For this case of matrix **A** of Eq. (2.3) is in general:

$$\mathbf{A} = \begin{pmatrix} a_1 & a_2 \\ b_1 & b_2 \end{pmatrix} \tag{A.1}$$

where a_1 is the arc length of ray a in box 1, b_1 is the arc length of ray b in box 1, and similarly for a_2 and b_2. The singular values of **A** are the positive square roots of the eigenvalues of the matrix $\mathbf{AA}^{\mathrm{T}}$:

$$\mathbf{AA}^{\mathrm{T}} = \begin{pmatrix} a_1^2 + a_2^2 & a_1b_1 + a_2b_2 \\ a_1b_1 + a_2b_2 & b_1^2 + b_2^2 \end{pmatrix}. \tag{A.2}$$

Thus the two singular values for **A** are:

$$\lambda_{\pm} = (2)^{-1/2}\{(a_1^2 + a_2^2 + b_1^2 + b_2^2) \pm [(a_1^1 + a_2^2 - b_1^2 - b_2^2)^2 + 4(a_1b_1 + a_2b_2)^2]^{1/2}\}^{1/2}. \tag{A.3}$$

The arc lengths in each box, such as a_1, are non-linear functions of the source, and receiver location, as well as the box geometry. The singular values are also nonlinear functions of the arc lengths a_1, a_2, b_1 and b_2. This non-linearity persists if the arc lengths in (A.3) are rewritten in terms of the source and receiver locations, and box geometry. The order of the equations (A.3) becomes higher for models with more boxes and more rays.

REFERENCES

Behringer, D., T. Birdsall, M. Brown, B. Cornuelle, R. Heinmiller, R. Knox, K. Metzger, W. Munk, J. Spiesberger, R. Spindel, D. Webb, P. Worcester and C. Wunsch, 1982: A demonstration of ocean acoustic tomography. *Nature,* **299,** 121–125.

Bennett, A., 1985: Array design by inverse methods. *Progress in Oceanography,* Vol. 15, Pergamon, 129–156.

Bretherton, F. P., R. E. Davis and C. B Fandry, 1976: A technique for objective analysis and design of oceanographic experiments applied to MODE-73. *Deep-Sea Res.,* **23,** 559–582.

——, and J. C. McWilliams, 1980: Estimations from irregular arrays. *Rev. Geophys. Space Phys.,* **18,** 789–812.

Cornuelle, B., W. Munk and P. Worcester, 1989: Ocean acoustic tomography from ships. *J. Geophys. Res.*, **94,** 6232–6250.

Davidson, W. C., 1959: Variable metric methods for minimization. A. E. C. Res. and Develop. Report ANL-5990, Argonne National Laboratory, Argonne, Illinois.

Eisler, T. J., R. New and D. Calderone, 1982: Resolution and variance in acoustic tomography. *J. Acoust. Soc. Amer.*, **72,** 1965–1977.

Geman, S., and D. Geman, 1984: Stochastic relaxation, Gibbs distributions, and the bayesian restoration of images. *IEEE Trans. on Pattern Analysis and Machine Intelligence,* **PAMI-6,** 721–741.

Gill, P. E., W. Murray and M. H. Wright, 1981: *Practical Optimization.* Academic Press.

Kirkpatrick, S., C. Gelatt and M. Vecchi, 1983: Optimization by simulated annealing. *Science,* **220,** 671–680.

Kumar, S., and J. H. Seinfeld, 1978: Optimal location of measurements for distributed parameter estimation. *IEEE Trans. Autom. Control,* **AC-23,** 690–698.

Lanczos, C., 1961: *Linear Differential Operators.* Van Nostrand, 564 pp.

Langstaff J., C. Seigneur, M. Liu, J. Behar and J. McElroy, 1986: Design of an optimum air monitoring network for exposure assessments. *Atmos. Environ.*, **21,** 1393–1410.

Munk, W., and C. Wunsch, 1979: Ocean acoustic tomography: A scheme for large scale monitoring. *Deep–Sea Res.*, **26A,** 123–161.

Murtagh, B. A., and M. A. Saunders, 1983: MINOS 5.0 user's guide. Technical report SOL 83-20, Systems optimization laboratory, Department of operations research, Stanford University, Stanford, California 94305.

Press, W., B. Flannery, S. Teukolsky, and W. Vetterling, *Numerical Recipes: The Art of Scientific Computing.* Cambridge University Press, 818 pp.

Schröter, J., and C. Wunsch, 1986: Solution of nonlinear finite difference ocean models by optimization methods with sensitivity and observational strategy analysis. *J. Phys. Oceanogr.*, **16,** 1855–1874.

Seber, G. A., 1977: *Linear Regression Analysis.* John Wiley, 465 pp.

Wolfe, P., 1962: The reduced-gradient method. Unpublished manuscript, RAND Corporation.